1988ApJ...332..261D

THE ASTROPHYSICAL JOURNAL, 332:261–270, 1988 September 1

THE EQUATION OF STATE FOR STELLAR ENVELOPES. III. THERMODYNAMIC QUANTITIES

WERNER DÄPPEN,[1] DIMITRI MIHALAS,[1,2,3] D. G. HUMMER,[3,4]
AND BARBARA WEIBEL MIHALAS[2,5]

Received 1987 March 30; accepted 1988 February 29

ABSTRACT

We derive general formulae for the computation of the thermodynamic properties of a partially ionized (and/or dissociated) multicomponent gas in terms of second derivatives of the free energy with respect to temperature, volume, and occupation numbers. For the free energy used in our previous work we give explicit analytical expressions for all derivatives required to construct the thermodynamic quantities.

Representative results for several different thermodynamic properties of a hydrogen-helium plasma with $N(\mathrm{He})/N(\mathrm{H}) = 0.10$ are presented as color plots, which make the qualitative behavior of the results readily comprehensible over a large temperature-density domain.

Subject headings: atomic processes — equation of state — stars: interiors

I. INTRODUCTION

At the temperatures and low-to-moderate densities characteristic of stellar envelopes, the free-energy minimization technique (Graboske, Harwood, and Rogers 1969; Fontaine, Graboske, and Van Horn 1977) provides a powerful formalism for the computation of the equation of state, and associated thermodynamic quantities, of stellar material. Such thermodynamic quantities are often needed in stellar evolution calculations, particularly when convection is present. They also appear prominently in linear pulsation analyses. In both of these applications it is desirable to have smooth variations of any thermodynamic property as a function of ρ and T. This requirement is even stronger for certain helioseismological applications where one needs the *derivatives* of thermodynamic quantities. In what follows we describe a method by which the astrophysically interesting thermodynamic properties themselves can be evaluated from analytical formulae, resulting in data that are smooth enough to survive a numerical differentiation to give the data needed for helioseismology with reasonable accuracy.

In previous papers we have developed a completely analytical (and differentiable) expression for the free energy of a partially ionized gas, in which smooth and differentiable internal partition functions are obtained through use of an occupation probability formalism (Hummer and Mihalas 1988, hereafter Paper I; Mihalas, Däppen, and Hummer 1988, hereafter Paper II). We showed in Paper II that in the low-density regime the computed ionization fractions approach those obtained from a Saha equilibrium based on internal partition functions that use all atomic levels in the dataset. In the high-density regime the ionization fractions approach a Saha equilibrium obtained using only ground states in the internal partition functions, until finally pressure ionization or dissociation occurs at some characteristic density and the two sets of results diverge from one another. Our formalism can describe pressure dissociation of molecules in a neutral gas and pressure ionization of atoms and ions in an ionized plasma reasonably well, although it might already be beyond its domain of applicability. But to obtain pressure ionization of atoms in a neutral gas at relatively low temperatures and very high densities we were forced to modify the formalism by introducing an additional free energy term patterned after that used in calculations of interacting hard spheres.

The purpose of this paper is threefold: (1) we describe a method for deriving general expressions for all thermodynamic quantities of interest (e.g., specific heats) in terms of derivatives of the free energy; (2) for our adopted free energy we give explicit analytical formulae for all derivatives required in the evaluation of these quantities; (3) we show some representative results for a hydrogen-helium mixture.

II. ANALYSIS

All second-order thermodynamic properties of a gas (e.g., specific heats, adiabatic exponents, compressibility, thermal expansion coefficient, etc.) can be computed from given values for any three of them (Cox and Giuli 1968, pp. 211–214). A convenient choice for the basic three is the specific heat at constant volume

$$c_V \equiv \frac{T}{\rho}\left(\frac{\partial S}{\partial T}\right)_V , \tag{1}$$

where S is the entropy of the gas, and the first derivatives of the gas pressure with respect to temperature and density

$$\chi_T \equiv \left(\frac{\partial \ln p}{\partial \ln T}\right)_\rho , \tag{2}$$

---

[1] High Altitude Observatory, National Center for Atmospheric Research. NCAR is sponsored by the National Science Foundation.
[2] Department of Astronomy, University of Illinois.
[3] Joint Institute for Laboratory Astrophysics, University of Colorado and National Bureau of Standards.
[4] Staff Member, Quantum Physics Division, National Bureau of Standards.
[5] National Center for Supercomputing Applications, University of Illinois.

and

$$\chi_\rho \equiv \left(\frac{\partial \ln p}{\partial \ln \rho}\right)_T . \tag{3}$$

Note that in these partial derivatives the "external" concentration variables (total numbers of nuclei of each chemical species) are kept fixed, but "internal" variables (ionization degrees) are allowed to vary in the differentiation process. To illustrate the procedure, we derive an explicit expression for c_V.

Express the free energy F as a function of T, V, and a set of *reaction parameters* (Reichl 1980, p. 72):

$$\boldsymbol{\lambda} \equiv (\lambda_1, \lambda_2, \ldots, \lambda_n) , \tag{4}$$

where n is the number of chemical reaction equations (stochlometric relations) describing the system. These parameters are defined such that an ionization-recombination (or dissociation-recombination) event changes one of them by one unit. Thus the stochlometric constraints are automatically incorporated by use of these parameters, which is very convenient. Then for each choice of (T, V) the free energy $F(T, V, \boldsymbol{\lambda})$ is minimized with respect to variations in $\boldsymbol{\lambda}$ to find the equilibrium values $\boldsymbol{\lambda}^{\text{eq}}(T, V)$ from

$$\boldsymbol{\mu}[T, V, \boldsymbol{\lambda}^{\text{eq}}(T, V)] \equiv \left(\frac{\partial F}{\partial \boldsymbol{\lambda}}\right)_{T,V}\Bigg|_{\boldsymbol{\lambda} = \boldsymbol{\lambda}^{\text{eq}}(T,V)} = 0 . \tag{5}$$

To calculate c_V we can use the relation $S = -(\partial F/\partial T)_V$ to write

$$c_V = -\frac{T}{\rho}\left(\frac{\partial^2 F}{\partial T^2}\right)_V . \tag{6}$$

However, in evaluating equation (6) we must be careful to remember that the derivative is at constant V, but not at constant $\boldsymbol{\lambda}$ because $\boldsymbol{\lambda}^{\text{eq}}$ is a function of T and V. Thus to clarify the analysis, define the new function

$$\hat{F}(T, V) \equiv F[T, V, \boldsymbol{\lambda}^{\text{eq}}(T, V)] , \tag{7}$$

so that

$$c_V = -\frac{T}{\rho}\left(\frac{\partial^2 \hat{F}}{\partial T^2}\right)_V . \tag{8}$$

Then

$$\left(\frac{\partial \hat{F}}{\partial T}\right)_V = \left(\frac{\partial F}{\partial T}\right)_{V,\boldsymbol{\lambda}} + \left(\frac{\partial F}{\partial \boldsymbol{\lambda}}\right)_{T,V}\left(\frac{\partial \boldsymbol{\lambda}^{\text{eq}}}{\partial T}\right)_V = \left(\frac{\partial F}{\partial T}\right)_{V,\boldsymbol{\lambda}} , \tag{9}$$

where the second step follows from equation (5). Further,

$$\left(\frac{\partial^2 \hat{F}}{\partial T^2}\right)_V = \left(\frac{\partial^2 F}{\partial T^2}\right)_{V,\boldsymbol{\lambda}} + \left(\frac{\partial^2 F}{\partial T\, \partial \boldsymbol{\lambda}}\right)_V\left(\frac{\partial \boldsymbol{\lambda}^{\text{eq}}}{\partial T}\right)_V . \tag{10}$$

To calculate $(\partial \boldsymbol{\lambda}^{\text{eq}}/\partial T)_V$, we differentiate equation (5) with respect to T, obtaining

$$\left(\frac{\partial^2 F}{\partial \boldsymbol{\lambda}\, \partial T}\right)_V + \left(\frac{\partial^2 F}{\partial \boldsymbol{\lambda}^2}\right)\left(\frac{\partial \boldsymbol{\lambda}^{\text{eq}}}{\partial T}\right)_V \equiv 0 , \tag{11}$$

whence

$$\left(\frac{\partial \boldsymbol{\lambda}^{\text{eq}}}{\partial T}\right)_V = -\left(\frac{\partial^2 F}{\partial \boldsymbol{\lambda}^2}\right)^{-1}\left(\frac{\partial^2 F}{\partial T\, \partial \boldsymbol{\lambda}}\right)_V . \tag{12}$$

All quantities on the right-hand side of equation (12) are to be evaluated at $\boldsymbol{\lambda} = \boldsymbol{\lambda}^{\text{eq}}$.

Combining equations (8), (10), and (12), we obtain finally

$$c_V = -\frac{T}{\rho}\left[\left(\frac{\partial^2 F}{\partial T^2}\right)_{V,\boldsymbol{\lambda}} - \left(\frac{\partial^2 F}{\partial T\, \partial \boldsymbol{\lambda}}\right)_V\left(\frac{\partial^2 F}{\partial \boldsymbol{\lambda}^2}\right)^{-1}_{T,V}\left(\frac{\partial^2 F}{\partial T\, \partial \boldsymbol{\lambda}}\right)_V\right] . \tag{13}$$

By a similar analysis starting from $p = -(\partial F/\partial V)_{\boldsymbol{\lambda},T}$, we have

$$\chi_T = -\frac{T}{p}\frac{\partial}{\partial T}\left[\left(\frac{\partial F}{\partial V}\right)_{T,\boldsymbol{\lambda}}\right]_V \tag{14a}$$

and

$$\chi_\rho = \frac{V}{p}\frac{\partial}{\partial V}\left[\left(\frac{\partial F}{\partial V}\right)_{T,\boldsymbol{\lambda}}\right]_T , \tag{14b}$$

whence

$$\chi_T = -\frac{T}{p}\left[\left(\frac{\partial^2 F}{\partial T\,\partial V}\right)_\lambda - \left(\frac{\partial^2 F}{\partial V\,\partial \boldsymbol{\lambda}}\right)_T \left(\frac{\partial^2 F}{\partial \boldsymbol{\lambda}^2}\right)^{-1}_{T,V} \left(\frac{\partial^2 F}{\partial T\,\partial \boldsymbol{\lambda}}\right)_V\right] \tag{15}$$

and

$$\chi_p = \frac{V}{p}\left[\left(\frac{\partial^2 F}{\partial V^2}\right)_{T,\lambda} - \left(\frac{\partial^2 F}{\partial V\,\partial \boldsymbol{\lambda}}\right)_T \left(\frac{\partial^2 F}{\partial \boldsymbol{\lambda}^2}\right)^{-1}_{T,V} \left(\frac{\partial^2 F}{\partial V\,\partial \boldsymbol{\lambda}}\right)_T\right] . \tag{16}$$

Explicit analytical expressions for $(\partial^2 F/\partial T^2)$, $(\partial^2 F/\partial T\,\partial V)$, and $(\partial^2 F/\partial V^2)$ are given in the Appendix. Notice that equations (13), (15), and (16) contain derivatives with respect to reaction parameters, whereas the free-energy minimization procedure of Paper II provides derivatives with respect to occupation numbers. The former are easily derived from the latter via a transformation matrix **A**:

$$\frac{\partial F}{\partial \lambda_i} = \frac{\partial n_j}{\partial \lambda_i}\frac{\partial F}{\partial n_j} \equiv A_{ij}\frac{\partial F}{\partial n_j} , \tag{17}$$

or

$$\frac{\partial F}{\partial \boldsymbol{\lambda}} = \mathbf{A} \cdot \frac{\partial F}{\partial \boldsymbol{n}} . \tag{18}$$

(In eq. [17] the Einstein summation convention is used.) Similarly

$$\left(\frac{\partial^2 F}{\partial T\,\partial \boldsymbol{\lambda}}\right)_V = \mathbf{A} \cdot \left(\frac{\partial^2 F}{\partial T\,\partial \boldsymbol{n}}\right)_V , \tag{19}$$

$$\left(\frac{\partial^2 F}{\partial V\,\partial \boldsymbol{\lambda}}\right)_T = \mathbf{A} \cdot \left(\frac{\partial^2 F}{\partial V\,\partial \boldsymbol{n}}\right)_T , \tag{20}$$

and

$$\left(\frac{\partial^2 F}{\partial \boldsymbol{\lambda}^2}\right)_{T,V} = \mathbf{A} \cdot \left(\frac{\partial^2 F}{\partial \boldsymbol{n}^2}\right)_{T,V} \cdot \mathbf{A}^T . \tag{21}$$

Explicit analytical expressions for all of the derivatives appearing on the right-hand sides of equations (19)–(21) are given in the Appendix.

It is straightforward to choose appropriate reaction parameters and to construct the transformation matrix. Thus for hydrogen (which can both ionize and form molecules) one takes

$$N_{\mathrm{H}_2} = \lambda_{1\mathrm{H}} , \tag{22a}$$

$$N_{\mathrm{H}_2+} = \lambda_{2\mathrm{H}} , \tag{22b}$$

$$N_{\mathrm{H}-} = \lambda_{3\mathrm{H}} , \tag{22c}$$

$$N_p = \lambda_{4\mathrm{H}} - \lambda_{2\mathrm{H}} , \tag{22d}$$

$$N_{\mathrm{H}} = \alpha_{\mathrm{H}} N_{\mathrm{tot}} - 2\lambda_{1\mathrm{H}} - \lambda_{2\mathrm{H}} - \lambda_{3\mathrm{H}} - \lambda_{4\mathrm{H}} . \tag{22e}$$

Here N_{tot} is the total number of nuclei in the gas, and α_{H} is the (number) fraction of them that are hydrogen. For chemical element k with J_k ionization stages (but no molecules) one takes

$$N_{1k} = \alpha_k N_{\mathrm{tot}} - \lambda_{1k} , \tag{23a}$$

$$N_{2k} = \lambda_{1k} - \lambda_{2k} , \tag{23b}$$

$$N_{Jk} = \lambda_{J-1,k} . \tag{23c}$$

Then the number of electrons is

$$N_e = \lambda_{4\mathrm{H}} - \lambda_{3\mathrm{H}} + \sum_{k \neq \mathrm{H}} \sum_{j=1}^{J_{k-1}} \lambda_{jk} . \tag{24}$$

The elements of A_{ij} can be written down from equations (22)–(24) by inspection.

Then, given c_V, χ_T, and χ_ρ, all other thermodynamic quantities of interest follow from the standard relations (Cox and Giuli 1968):

$$c_p = c_V + \frac{p}{\rho T} \frac{\chi_T^2}{\chi_\rho} , \tag{25a}$$

$$\Gamma_3 - 1 = \frac{p}{\rho T} \frac{\chi_T}{c_V} , \tag{25b}$$

$$\Gamma_1 = \chi_T(\Gamma_3 - 1) + \chi_\rho , \tag{25c}$$

$$\frac{\Gamma_2}{\Gamma_2 - 1} = \frac{\Gamma_1}{\Gamma_3 - 1} , \tag{25d}$$

and

$$Q = \chi_T/\chi_\rho . \tag{25e}$$

Finally, it should be noted that because all of the derivatives entering into the computation of c_V, χ_T, and χ_ρ (and, of course, the other quantities defined in eq. [25]) are analytical and smooth, higher order derivatives; e.g., $(\partial\Gamma/\partial T)$ and $(\partial\Gamma/\partial\rho)$ can safely be computed by numerical differentiation.

III. RESULTS AND DISCUSSION

In this section we present some representative results for a hydrogen-helium gas having $N(\mathrm{He})/N(\mathrm{H}) = 0.10$. The effects of radiation were ignored in Paper II because there we concentrated exclusively on the ionization/recombination behavior of the material component of the gas. Here, in contrast, we examine the behavior of a *radiating fluid* (material plus radiation); hence, we account fully for the free energy of thermal-equilibrium radiation in the calculation of all thermodynamic quantities (see § V of the Appendix). Nevertheless, in some of the plots shown below our purpose is to display the behavior of the material component of the gas only; hence, we remove radiation effects "after the fact."

The second-order thermodynamic quantities provide a valuable means of making a stringent test of both the logical structure (i.e., freedom from bugs) and the numerical accuracy of the code because they can be computed two entirely independent ways: (*a*) by direct numerical differentiation of primary variables, as in equations (1)–(3), and (*b*) by use of higher order analytical derivatives of the free energy, as in equations (13), (15), and (16). We carried out several tests of this kind by computing several clusters of five isotherms, consisting of a central isotherm and four others offset by $\pm\Delta T$ and $\pm\Delta\rho$ relative to it. We verified that for c_V, χ_T, and χ_ρ we could obtain agreement between the two methods to about 1 part in 10^9, and that the error in the results obtained from numerical differencing grew as one expects for truncation errors. We think that these tests show that the code is essentially free of coding errors that can affect results of physical interest; of course, the *accuracy* of the results is set by limitations of the underlying physical models, not by numerics.

Color plots of a dozen thermodynamic properties of the gas are shown in Figure 1 (Plates 1–3). Results were computed for log $T = 3.5\ (0.02)\ 7.0$ and log $\rho = -10\ (0.10)\ 2.0$, and the colors of pixels were determined by bilinear interpolation in the cells defined by the computational grid. The gray areas in the lower right-hand corners of the plots (the same for all of them) are used to delete results deemed to be physically unreliable (despite the fact that the code converged to an answer).

Figures 1*a*–1*d* show the logarithms of the occupation fraction of H_2, neutral H, neutral He, and He^+, respectively. (For ionization stage j of chemical element k, $f_{jk} \equiv N_{jk}/\sum_j N_{jk}$). In the plots red corresponds to $f = 1$, and violet to $f \leq 10^{-6}$. Figure 1*a* shows that at low temperatures and moderate densities all the hydrogen is in the form of H_2. At fixed density, H_2 dissociates into neutral H with increasing temperature. At fixed temperature, f_{H_2} increases with density until log $\rho \sim -1$, where pressure dissociation occurs and H_2 is rapidly converted into neutral H. Figure 1*b* shows the fraction of neutral H. At low enough temperatures H is depleted to form H_2; hence, the maximum f_H lies along a ridge line running from log $T \sim 3.5$ near log $\rho \sim -10$ to log $T \sim 4.25$ for log $\rho \sim -1$. The stair-step effects seen near the right edge of the red region is a plotting artifact resulting from using too coarse a computational grid to resolve the rapid variation of f_H with ρ. Figure 1*c* for neutral He shows qualitatively the same phenomena as Figure 1*a* for H_2. There are, of course, major quantitative differences in that at fixed density He persists to much higher temperatures because of its large ionization potential, and at fixed temperature to much higher densities because of its small atomic radius. Likewise, Figure 1*d* for He^+ shows qualitatively the same behavior as Figure 1*b* for H: the recombination locus of He^+ into He runs from log $T \sim 4.2$ for log $\rho \sim -10$ to log $T \sim 4.75$ for log $\rho \sim 0$; the ionization locus of He^+ into He^{++} runs from log $T \sim 4.6$ to log $T \sim 5.5$ for log $\rho \sim 0$; pressure ionization to He^{++} occurs for log $\rho \sim 1$; and maximum f_{He^+} runs along a ridge line from log $T \sim 4.5$ for log $\rho \sim -10$ to log $T \sim 5$ for log $\rho \sim 0$.

Figure 1*e* shows a plot of $\Pi \equiv p_{\mathrm{gas}}\,\mu_0\,m_0/\rho kT$, the ratio of the actual gas pressure (material component only) to the pressure of an ideal monatomic gas with the same number of nuclei per unit volume. Here m_0 is one atomic mass unit, and the "molecular weight" is $\mu_0 = \sum_k \alpha_k A_k$, where k ranges over all chemical elements of atomic weight A_k and fractional number abundance α_k (normalized such that $\sum_k \alpha_k = 1$). The blue region at the bottom of the plot corresponds to $\Pi = 0.5$, the appropriate value for a gas composed dominantly of H_2. At higher temperatures, where H_2 is dissociated but H has not yet ionized, Π goes to 1.0, the ideal value for monatomic gases. At yet higher temperatures, H ionizes; hence, $\Pi \rightarrow 2$ (two free particles per unit mass). For log $\rho \approx -1$ and log $T \leq 4.75$, where pressure ionization occurs Π takes on very large values (dark red region), reflecting the very powerful and stiff interaction occurring among particles as electrons are crushed out of atoms by the hard sphere (including the additional pressure ionization term of Paper II) and Coulomb interaction terms in the occupation probability factors contained in F_2. Finally, the

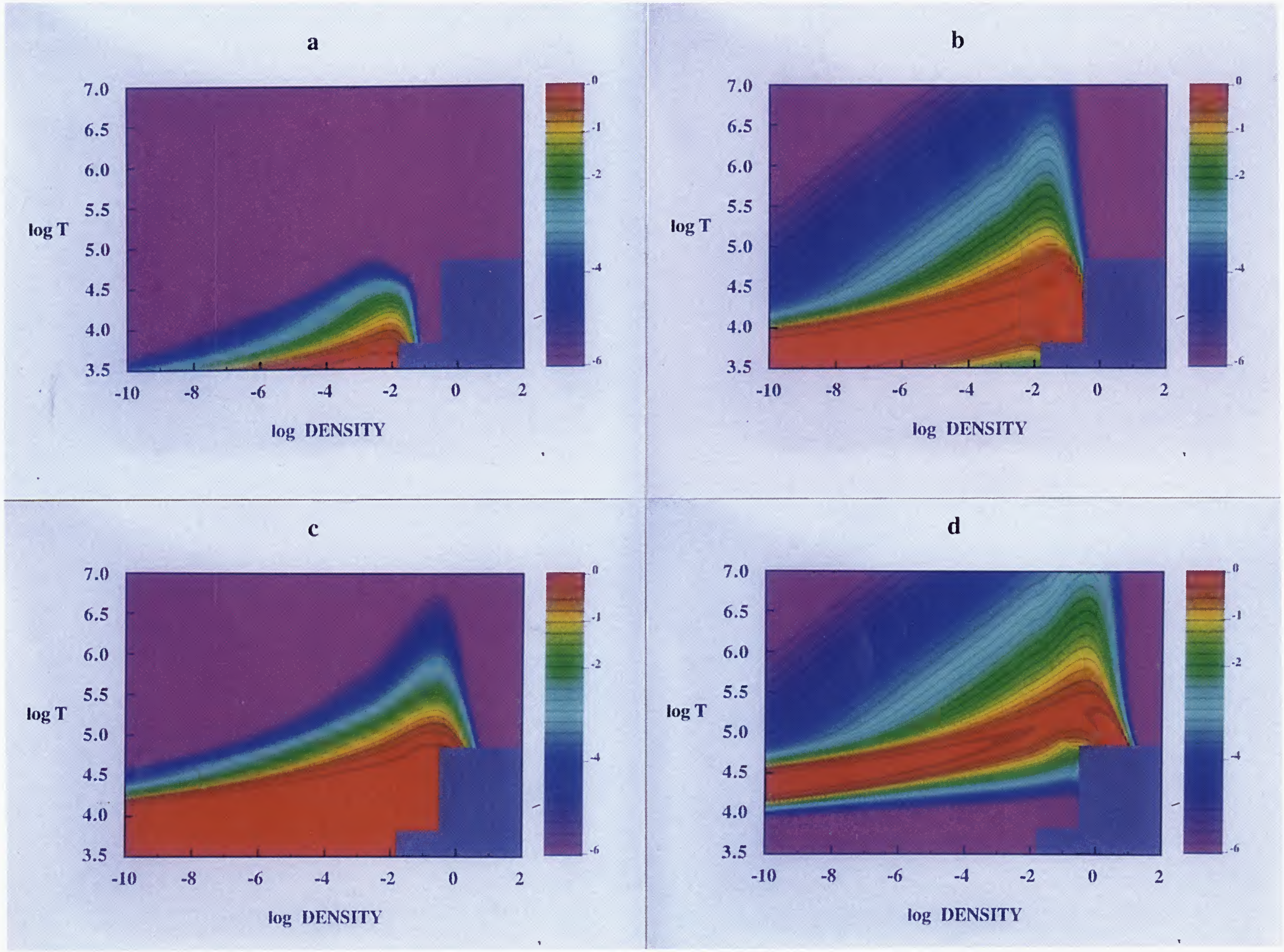

FIG. 1.—Variation of thermodynamic properties of a hydrogen—helium mix, $N(\mathrm{He})/N(\mathrm{H}) = 0.1$, over a domain in the (ρ, T)-plane. Ordinate is $\log T$, and abscissa is $\log \rho$. Values of the variables plotted are coded by color according to the chart at the right-hand edge of the plot. The gray area in the lower right-hand corner blocks the region where the validity of the physical theory becomes doubtful (even though the code was able to converge to qualitatively reasonable results in most cases). (*a*) $\log f_{\mathrm{H}_2}$; (*b*) $\log f_{\mathrm{H}}$; (*c*) $\log f_{\mathrm{He}}$; (*d*) $\log f_{\mathrm{He}^+}$; (*e*) $\rho_{\mathrm{gas}} \mu_0 m_0/\rho kT$; (*f*) $E_{\mathrm{gas}} \mu_0 m_0/\rho kT$; (*g*) $N_e \mu_0 m_0/\rho$; (*h*) c_v (gas) per particle; (*i*) Γ_1; (*j*) $(\Gamma_2 - 1)/\Gamma_2$; (*k*) χ_ρ; (*l*) χ_T.

DÄPPEN *et al.* (*see* **332**, 264)

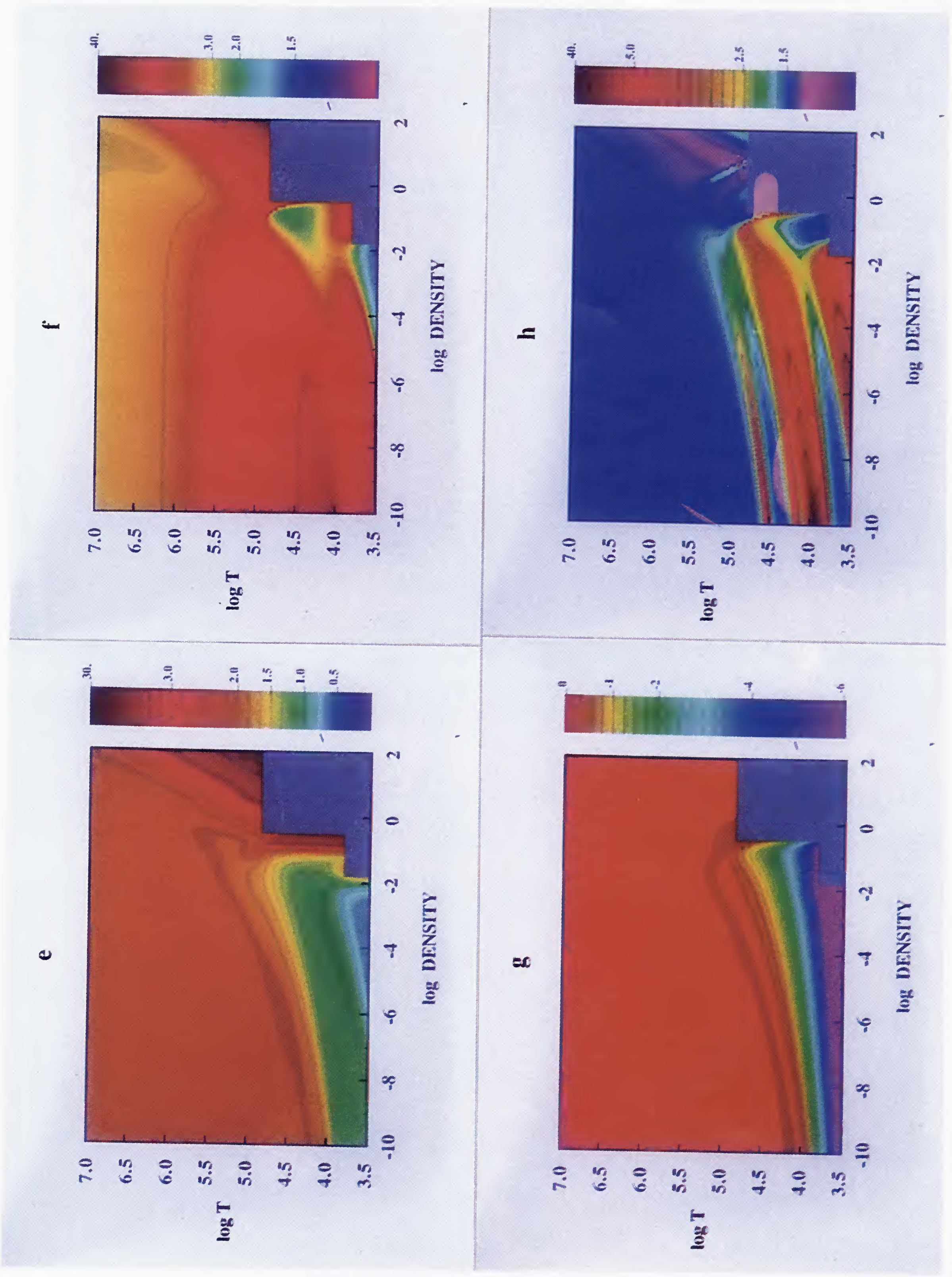

FIG. 1—*Continued*

DÄPPEN *et al.* (*see* **332**, 264)

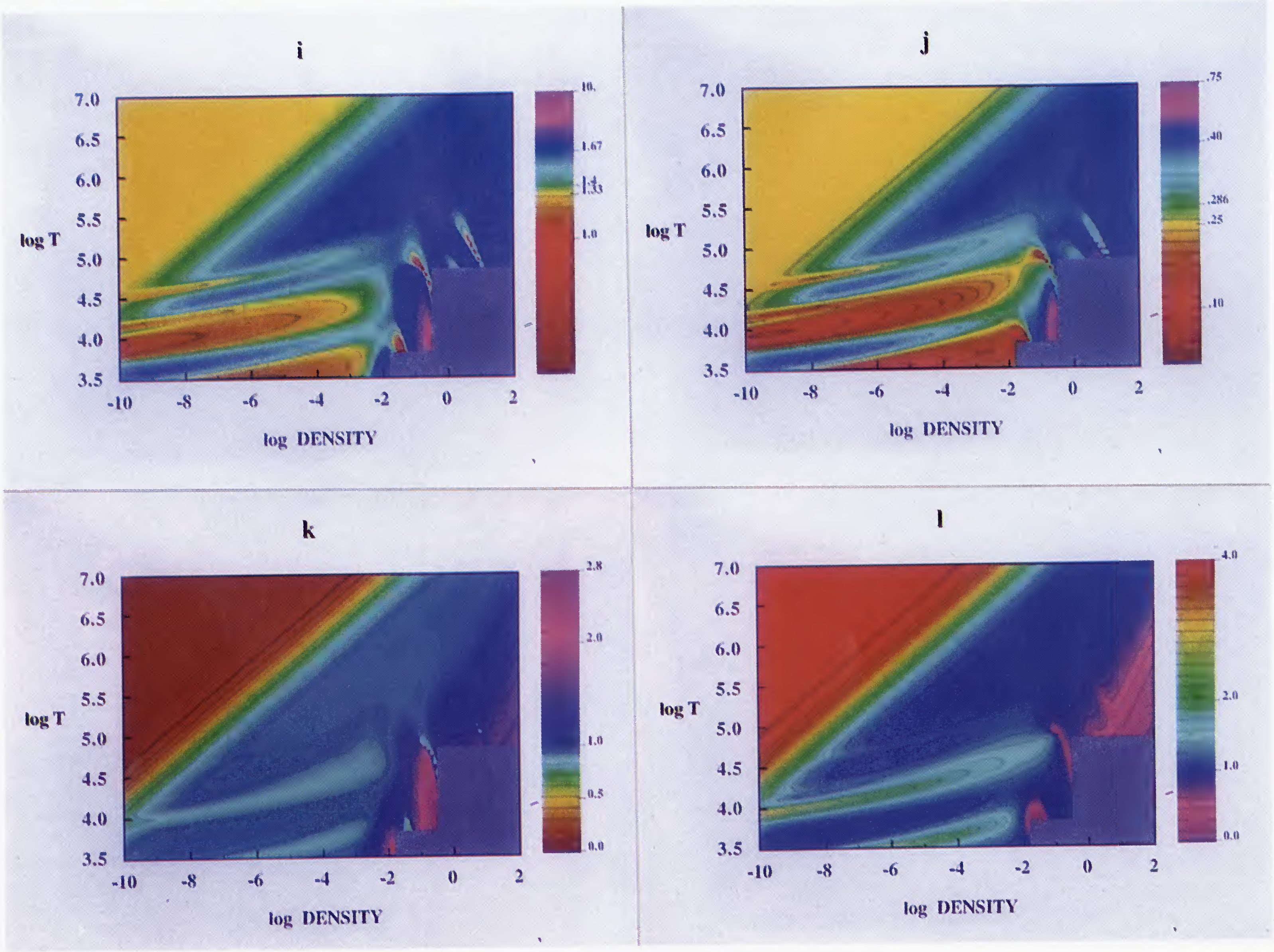

FIG. 1—*Continued*

DÄPPEN *et al.* (*see* **332**, 264)

1988ApJ...332..261D

diagonal red contours at the right-hand edge of the plot show the well-known nonclassical increase in pressure produced by electron degeneracy.

Figure 1*f* is a plot of $\tilde{e} \equiv E_{\text{gas}} \mu_0 m_0/\rho kT$, the internal energy per particle, in units of kT (material component of the gas only). Energies are measured upward from the ground state of H_2 for hydrogen and from the ground state of neutral He for helium. For most of the diagram, the internal excitation energy plus the energies of dissociation and ionization associated with the particles far outweigh their translational energies; hence, $\tilde{e}$ is much larger than the ideal monatomic gas value $\tilde{e} = 3/2$. The maximum in $\tilde{e}$ occurs for $4.0 \leq \log T \leq 4.5$ and $-10 \leq \log \rho \leq -6$, where both neutral H and neutral He are ionizing strongly and are also fairly highly excited. Only at very high temperatures ($\log T \gtrsim 6$) does the translational energy dominate so that we get $3kT/2$ per particle, but have essentially two particles per unit mass (i.e., a proton and an electron) so that $\tilde{e}$ approaches 3.0. At the right-hand edge of the plot we see diagonal contours that result from the contribution of electron degeneracy to the total internal energy of the gas.

Figure 1*g* is a plot of the logarithm of the number of free electrons per heavy particle (nucleus), $N_e \mu_0 m_0/\rho$. In the limit of complete ionization this ratio equals 1.1 for our mixture. The plot shows the expected smooth increase in ionization with increasing temperature at fixed density, and, at fixed temperature, the expected effects of thermal ionization at low densities, and of pressure ionization at high densities. A plot of the proton occupation fraction f_p is very similar to this figure because hydrogen is the dominant electron donor.

Figure 1*h* is a plot of $\tilde{c}_V = \rho c'_V/(N_n + N_e)k$, the specific heat at constant volume of the material component of the gas only (c'_V) per particle (N_e is the number of electrons; N_n is the number of nuclei), in units of Boltzmann's constant. The figure shows clearly that $\tilde{c}_V$ reaches huge values in the H_2 dissociation domain (at the bottom edge of the plot); in the H and He ionization domains, which essentially run together (being only slightly separated near $\log T = 4.1$ at $\log \rho = -10$); and in the He^+ ionization domain. In each case an input of thermal energy gets locked up into potential energy (i.e., energy of excitation, dissociation, or ionization) in the gas instead of producing a rise in temperature; hence, the specific heat (heat input per unit temperature change) is large. The classical value $\tilde{c}_V = 3/2$ is attained only when the gas is completely ionized (upper portion of plot) and in the blue regions between the major ionization domains. At the right-hand edge of the plot $\tilde{c}_V$ drops below the classical value when electron degeneracy becomes important. The red ridge line extending from the thermal ionization domain of H into the gray area near $\log T = 4$, and $\log \rho = -0.5$ reveals a narrow region of large $\tilde{c}_V$ resulting from pressure ionization of hydrogen; the stair-step shape of this feature is an artifact of underresolution from use of too coarse a computational grid. At the top edge of the gray area we see additional features resulting from pressure ionization of He (small blue area at $\log \rho \approx 0$) and of He^+ (sharp ridge line extending upward and to left at $\log \rho \approx 1$). Again the disintegration of the ridge line into a series of "islands" is an artifact of underresolution by the computational grid.

Figures 1*i* and 1*j* show, respectively, Γ_1 and $(\Gamma_2 - 1)/\Gamma_2$ for the gas composed of material particles plus radiation. In many respects both of these plots are similar to Figure 1*h*. The H_2 thermal dissociation region, and the H, He, and He^+ thermal ionization regions, where Γ_1, Γ_2, and Γ_3 all approach unity, appear prominently; in particular, the $He \leftrightarrow He^+$ region appears much more clearly in these plots than in Figure 1*h*. Likewise the H, He, and He^+ pressure ionization regions (where again the gammas tend toward unity) all stand out clearly, and the H_2 pressure dissociation region extending upward from $\log T = 3.75$ and $\log \rho = -1.5$ is seen clearly for the first time in Figure 1*i*. As before, we see some artifacts of underresolution in the plots of the pressure ionization features of H_2 and He^+. A new feature in these plots is the appearance of a large (yellow) region dominated by radiation in the low-density, high-temperature region of the plot (upper left corner). Here all gammas tend toward the limit $\gamma = 4/3$ appropriate for pure radiation.

Finally, Figures 1*k* and 1*l* show the behavior of $\chi_\rho \equiv (d \ln p/d \ln \rho)_T$ and $\chi_T \equiv (d \ln p/d \ln T)_\rho$, where p now includes radiation pressure in addition to the material gas pressure. We again see the prominent H_2 and H thermal dissociation and ionization regions, in which χ_ρ decreases noticeably below the ideal gas value (because an increase in density tends to produce recombination rather than a rise in pressure), while χ_T rises significantly above the ideal gas value (because a higher temperature tends to produce more particles, and therefore more pressure). In pressure ionization regions (violet) χ_ρ rises well above the classical value because both the hard-sphere and the Stark-ionization interaction terms in F_2 depend exponentially on density, and thus lead to a very steep response of p to ρ. In these same regions χ_T drops nearly to zero because the degree of ionization, the number of particles, and the free energy are all essentially independent of temperature in these domains. Likewise p is essentially independent of T; hence, $\chi_T \rightarrow 0$, in the domain of strong electron degeneracy (diagonal violet region at right-hand edge of plot). In the high-temperature, low-density regime (diagonal red region in upper left corner) the total pressure of the radiating fluid is independent of ρ and varies as T^4; hence, $\chi_\rho \rightarrow 0$ and $\chi_T \rightarrow 4$.

We remind the reader that all of the results shown in Figure 1 apply only to a hydrogen-helium mix. When other elements are included in the mix, a more complicated structure appears in all plots, although in most cases the amplitudes of the new features are small because elements other than H and He have such small abundances in normal stellar material. The situation could, of course, be quite different for material that has been heavily processed by thermonuclear reactions, but it would be straightforward to calculate the behavior of even exotic mixtures with the present code.

IV. PROSPECTS

For the present, we regard the code described here and in Paper II as being essentially completed. The primary use we will make of the code is to calculate stellar envelope opacities for ($3.5 \leq \log T \leq 7$, $-12 \leq \log \rho \leq -2$) in conjunction with the Opacity Project (see Paper I). In our opinion the code's internal consistency and precision have been adequately validated by the tests described in § III. We believe that it should perform reliably in the domain stated above (and also at higher densities at sufficiently high temperatures). While we will undoubtedly make changes in the atomic data as improved (and/or more complete) values become available, we do not, at the present time, envision making major changes in the formalism or underlying physics.

It is not our plan to publish large tables of results because such tables are cumbersome to use and consume valuable journal

1988ApJ...332..261D

space. We will, however, try to provide data on magnetic tape to interested parties, on request. Users of those data will need to develop their own interpolation routines; we suggest they consider using two-dimensional monotonized interpolants such as discussed by Carlson and Fritsch (1985). We can also attempt to provide clusters of isotherms suitable for numerical differentiation of quantities such as c_V, Γ, etc.

Because our code is designed mainly to construct complete isotherms, it requires adaptation in order to follow a specific track in the (ρ, T)-plane, say the temperature-density profile of the Sun. A more important limitation is that the code cannot easily handle changes in chemical composition along an isotherm. To deal with such situations one would need to construct several sets of tables with different compositions, and then perform an appropriate interpolation (several methods are discussed by Fontaine, Graboske, and Van Horn 1977); alternatively one would have to devise a robust starting procedure for the iteration process at an arbitrary (ρ, T). We have developed the code for a Cray X-MP because we expect to consider of the order of 200 particle species simultaneously. If one is content with a much smaller set of particle species, the code could probably be adapted to run on a mini- or microcomputer successfully.

We thank Carl J. Hansen for helpful comments on a draft of this paper. The computations were carried out at the National Center for Atmospheric Research and the National Center for Supercomputing Applications, both of which are sponsored by the National Science Foundation. This work was supported in part by National Aeronautics and Space Administration grant NAGW-766 to the University of Colorado and National Science Foundation grant AST 85-19209 to the University of Illinois. D. M. wishes to thank the Joint Institute for Laboratory Astrophysics for support as a Visiting Fellow during 1986–1987, when portions of this work were done.

APPENDIX

DERIVATIVES OF THE FREE ENERGY REQUIRED TO COMPUTE THERMODYNAMIC PROPERTIES

Below we summarize briefly analytical expressions for the derivatives needed to compute thermodynamic properties of the gas once the equilibrium occupation numbers $\{N_s\}$ have been found by minimizing $F(T, V, \{N_s\})$.

I. TRANSLATIONAL FREE ENERGY

$$-T^2 \frac{\partial}{\partial T}\left(\frac{F_1}{T}\right) = \frac{3}{2} kT \sum_{s \neq e} N_s = E_1 ; \tag{A1}$$

$$-\frac{\partial F_1}{\partial V} = \frac{kT}{V} \sum_{s \neq e} N_s = p_1 ; \tag{A2}$$

$$\frac{\partial^2 F_1}{\partial T^2} = -\frac{E_1}{T^2} ; \tag{A3}$$

$$\frac{\partial^2 F_1}{\partial T \partial V} = \frac{1}{T} \frac{\partial F_1}{\partial V} ; \tag{A4}$$

$$\frac{\partial^2 F_1}{\partial V^2} = -\frac{1}{V} \frac{\partial F_1}{\partial V} ; \tag{A5}$$

$$\frac{\partial^2 F_1}{\partial T \partial N_s} = \frac{1}{T} \frac{\partial F_1}{\partial N_s} - \frac{3}{2} k , \qquad s \neq e ; \tag{A6}$$

$$\frac{\partial^2 F_1}{\partial V \partial N_s} = -\frac{kT}{V} , \qquad s \neq e ; \tag{A7}$$

$$\frac{\partial^2 F_1}{\partial V \partial N_e} = \frac{\partial^2 F_1}{\partial T \partial N_e} \equiv 0 . \tag{A8}$$

II. INTERNAL FREE ENERGY

$$-T^2 \frac{\partial}{\partial T}\left(\frac{F_2}{T}\right) = \sum_{s \neq e} N_s \left[E_{1s} + \frac{1}{Z_s^*} \sum_i (E_{is} - E_{1s}) w_{is} g_{is} e^{-(E_{is} - E_{1s})/kT} \right] = E_2 ; \tag{A9}$$

$$-\frac{\partial F_2}{\partial V} = kT \sum_{s \neq e} \frac{N_s}{Z_s^*} \frac{\partial Z_s^*}{\partial V} = p_2 ; \tag{A10}$$

1988ApJ...332..261D

$$\frac{\partial^2 F_2}{\partial T^2} = -kT \sum_{s \neq e} \frac{N_s}{Z_s^*} \left[\frac{\partial^2 Z_s^*}{\partial T^2} + \left(\frac{2}{T} - \frac{1}{Z_s^*} \frac{\partial Z_s^*}{\partial T} \right) \frac{\partial Z_s^*}{\partial T} \right]; \tag{A11}$$

$$\frac{\partial^2 F_2}{\partial T \, \partial V} = -kT \sum_{s \neq e} \frac{N_s}{Z_s^*} \left[\frac{\partial^2 Z_s^*}{\partial T \, \partial V} + \left(\frac{1}{T} - \frac{1}{Z_s^*} \frac{\partial Z_s^*}{\partial T} \right) \frac{\partial Z_s^*}{\partial V} \right]; \tag{A12}$$

$$\frac{\partial^2 F_2}{\partial V^2} = -kT \sum_{s \neq e} \frac{N_s}{Z_s^*} \left[\frac{\partial^2 Z_s^*}{\partial V^2} - \frac{1}{Z_s^*} \left(\frac{\partial Z_s^*}{\partial V} \right)^2 \right]; \tag{A13}$$

$$\frac{\partial^2 F_2}{\partial T \, \partial N_r} = -kT \left\{ \frac{1}{T} \ln Z_r^* + \frac{1}{Z_r^*} \frac{\partial Z_r^*}{\partial T} + \sum_{s \neq e} \frac{N_s}{Z_s^*} \left[\frac{\partial^2 Z_s^*}{\partial T \, \partial N_r} + \left(\frac{1}{T} - \frac{1}{Z_s^*} \frac{\partial Z_s^*}{\partial T} \right) \frac{\partial Z_s^*}{\partial N_r} \right] \right\}, \qquad r \neq e; \tag{A14}$$

$$\frac{\partial^2 F_2}{\partial V \, \partial N_r} = -kT \left[\frac{1}{Z_r^*} \frac{\partial Z_r^*}{\partial V} + \sum_{s \neq e} \frac{N_s}{Z_s^*} \left(\frac{\partial^2 Z_s^*}{\partial V \, \partial N_r} - \frac{1}{Z_s^*} \frac{\partial Z_s^*}{\partial V} \frac{\partial Z_s^*}{\partial N_r} \right) \right], \qquad r \neq e. \tag{A15}$$

Here

$$\frac{\partial^2 Z_s^*}{\partial T^2} = \left(\frac{1}{kT^2} \right)^2 \sum_i (E_{is} - E_{1s})[(E_{is} - E_{1s}) - 2kT] w_{is} g_{is} e^{-(E_{is} - E_{1s})/kT}, \tag{A16}$$

$$\frac{\partial^2 Z_s^*}{\partial T \, \partial V} = -\frac{1}{kT^2 V} \sum_i (E_{is} - E_{1s})(\ln w_{is}) w_{is} g_{is} e^{-(E_{is} - E_{1s})/kT}, \tag{A17}$$

$$\frac{\partial^2 Z_s^*}{\partial V^2} = \frac{1}{V^2} \sum_i (\ln w_{is})(2 + \ln w_{is}) w_{is} g_{is} \, e^{-(E_{is} - E_{1s})/kT}, \tag{A18}$$

$$\frac{\partial^2 Z_s^*}{\partial N_r \, \partial T} = \frac{1}{kT^2} \sum_i (E_{is} - E_{1s}) \left(\frac{\partial \ln w_{is}}{\partial N_r} \right) w_{is} g_{is} e^{-(E_{is} - E_{1s})/kT}, \tag{A19}$$

and

$$\frac{\partial^2 Z_s^*}{\partial N_r \, \partial V} = -\frac{1}{V} \sum_i (1 + \ln w_{is}) \left(\frac{\partial \ln w_{is}}{\partial N_r} \right) w_{is} g_{is} e^{-(E_{is} - E_{1s})/kT}. \tag{A20}$$

All other derivatives are given in Appendix A of Paper II.

III. FREE ENERGY OF PARTIALLY DEGENERATE ELECTRONS

$$-\frac{\partial F_3}{\partial V} = \frac{N_e kT}{V} \frac{2}{3} \frac{F_{3/2}(\eta)}{F_{1/2}(\eta)} = p_3; \tag{A21}$$

$$-T^2 \frac{\partial}{\partial T} \left(\frac{F_3}{T} \right) = N_e kT \frac{F_{3/2}(\eta)}{F_{1/2}(\eta)} = E_3; \tag{A22}$$

$$\frac{\partial^2 F_3}{\partial T^2} = \frac{kN_e}{T} \left[\frac{9}{2} \frac{F_{1/2}(\eta)}{F_{-1/2}(\eta)} - \frac{5}{2} \frac{F_{3/2}(\eta)}{F_{1/2}(\eta)} \right]; \tag{A23}$$

$$\frac{\partial^2 F_3}{\partial T \, \partial V} = \frac{kN_e}{V} \left[3 \frac{F_{1/2}(\eta)}{F_{-1/2}(\eta)} - \frac{5}{3} \frac{F_{3/2}(\eta)}{F_{1/2}(\eta)} \right]; \tag{A24}$$

$$\frac{\partial^2 F_3}{\partial V^2} = -\frac{N_e kT}{V} \left(\frac{\partial \eta}{\partial V} \right); \tag{A25}$$

$$\frac{\partial^2 F_3}{\partial T \, \partial N_e} = k \left(\eta + T \frac{\partial \eta}{\partial T} \right); \tag{A26}$$

$$\frac{\partial^2 F_3}{\partial V \partial N_e} = kT \left(\frac{\partial \eta}{\partial V} \right); \tag{A27}$$

$$\frac{\partial^2 F_3}{\partial T \, \partial N_s} = \frac{\partial^2 F_3}{\partial V \, \partial N_s} \equiv 0, \qquad s \neq e. \tag{A28}$$

Here

$$\frac{\partial \eta}{\partial T} = -\frac{3}{T} \frac{F_{1/2}(\eta)}{F_{-1/2}(\eta)} = -\frac{3}{2} \frac{1}{T \theta_e}; \tag{A29}$$

$$\frac{\partial\eta}{\partial V} = -\frac{2}{V}\frac{F_{1/2}(\eta)}{F_{-1/2}(\eta)} = -\frac{1}{V\theta_e}\,; \tag{A30}$$

$$\frac{\partial^2\eta}{\partial T^2} = -\left[\frac{1}{T} + \frac{\theta'_e}{\theta_e}\left(\frac{\partial\eta}{\partial T}\right)\right]\left(\frac{\partial\eta}{\partial T}\right); \tag{A31}$$

$$\frac{\partial^2\eta}{\partial V^2} = -\left[\frac{1}{V} + \frac{\theta'_e}{\theta_e}\left(\frac{\partial\eta}{\partial V}\right)\right]\left(\frac{\partial\eta}{\partial V}\right); \tag{A32}$$

$$\frac{\partial^2\eta}{\partial T\,\partial V} = -\frac{\theta'_e}{\theta_e}\left(\frac{\partial\eta}{\partial T}\right)\left(\frac{\partial\eta}{\partial V}\right); \tag{A33}$$

$$\frac{\partial^2\eta}{\partial T\,\partial N_e} = -\frac{\theta'_e}{\theta_e}\left(\frac{\partial\eta}{\partial T}\right)\left(\frac{\partial\eta}{\partial N_e}\right); \tag{A34}$$

$$\frac{\partial^2\eta}{\partial T\,\partial N_s} \equiv 0\,, \qquad s \neq e\,, \tag{A35}$$

$$\frac{\partial^2\eta}{\partial V\,\partial N_e} = -\frac{\theta'_e}{\theta_e}\left(\frac{\partial\eta}{\partial V}\right)\left(\frac{\partial\eta}{\partial N_e}\right); \tag{A36}$$

and

$$\frac{\partial^2\eta}{\partial V\,\partial N_s} \equiv 0\,, \qquad s \neq e\,. \tag{A37}$$

All other quantities are defined in Appendix A of Paper II.

IV. CONFIGURATIONAL FREE ENERGY OF COULOMB INTERACTIONS

$$-T^2\frac{\partial}{\partial T}\left(\frac{F_4}{T}\right) = F_4\left(\frac{3}{2} - \frac{3}{2}\frac{TN_e\theta'_e}{\sum_\alpha N_\alpha Z_\alpha^2\theta_\alpha}\frac{\partial\eta}{\partial T} - \frac{\tau'}{\tau}\,T\,\frac{\partial x}{\partial T}\right) = E_4\,; \tag{A38}$$

$$-\frac{\partial F_4}{\partial V} = F_4\left(\frac{1}{2V} - \frac{3}{2}\frac{N_e\theta'_e}{\sum_\alpha N_\alpha Z_\alpha^2\theta_\alpha}\frac{\partial\eta}{\partial V} - \frac{\tau'}{\tau}\frac{\partial x}{\partial V}\right) = p_4\,; \tag{A39}$$

$$\begin{aligned}\frac{\partial^2F_4}{\partial T^2} = \frac{1}{F_4}\left(\frac{\partial F_4}{\partial T}\right)^2 + F_4\Bigg[\!\!\Bigg[\frac{1}{2T^2} + \left[\frac{\tau''}{\tau} - \left(\frac{\tau'}{\tau}\right)^2\right]\left(\frac{\partial x}{\partial T}\right)^2 + \left(\frac{\tau'}{\tau}\right)\frac{\partial^2x}{\partial T^2}\\ + \frac{3Ne}{2\sum_\alpha N_\alpha Z_\alpha^2\theta_\alpha}\left\{\theta''_e\left(\frac{\partial\eta}{\partial T}\right)^2 + \theta'_e\left[\frac{\partial^2\eta}{\partial T^2} - \frac{N_e\theta'_e}{\sum_\alpha N_\alpha Z_\alpha^2\theta_\alpha}\left(\frac{\partial\eta}{\partial T}\right)^2\right]\right\}\Bigg]\!\!\Bigg]\,;\end{aligned} \tag{A40}$$

$$\begin{aligned}\frac{\partial^2F_4}{\partial T\,\partial V} = \frac{1}{F_4}\left(\frac{\partial F_4}{\partial T}\right)\left(\frac{\partial F_4}{\partial V}\right) + F_4\Bigg[\!\!\Bigg[\left[\frac{\tau''}{\tau} - \left(\frac{\tau'}{\tau}\right)^2\right]\left(\frac{\partial x}{\partial V}\right)\left(\frac{\partial x}{\partial T}\right) + \left(\frac{\tau'}{\tau}\right)\frac{\partial^2x}{\partial T\,\partial V}\\ + \frac{3N_e}{2\sum_\alpha N_\alpha Z_\alpha^2\theta_\alpha}\left\{\theta''_e\left(\frac{\partial\eta}{\partial T}\right)\left(\frac{\partial\eta}{\partial V}\right) + \theta'_e\left[\frac{\partial^2\eta}{\partial T\,\partial V} - \frac{N_e\theta'_e}{\sum_\alpha N_\alpha Z_\alpha^2\theta_\alpha}\left(\frac{\partial\eta}{\partial T}\right)\left(\frac{\partial\eta}{\partial V}\right)\right]\right\}\Bigg]\!\!\Bigg]\,;\end{aligned} \tag{A41}$$

$$\begin{aligned}\frac{\partial^2F_4}{\partial V^2} = \frac{1}{F_4}\left(\frac{\partial F_4}{\partial V}\right)^2 + F_4\Bigg[\!\!\Bigg[\frac{1}{2V^2} + \left[\frac{\tau''}{\tau} - \left(\frac{\tau'}{\tau}\right)^2\right]\left(\frac{\partial x}{\partial V}\right)^2 + \left(\frac{\tau'}{\tau}\right)\frac{\partial^2x}{\partial V^2}\\ + \frac{3N_e}{2\sum_\alpha N_\alpha Z_\alpha^2\theta_\alpha}\left\{\theta''_e\left(\frac{\partial\eta}{\partial V}\right)^2 + \theta'_e\left[\frac{\partial^2\eta}{\partial V^2} - \frac{N_e\theta'_e}{\sum_\alpha N_\alpha Z_\alpha^2\theta_\alpha}\left(\frac{\partial\eta}{\partial V}\right)^2\right]\right\}\Bigg]\!\!\Bigg]\,;\end{aligned} \tag{A42}$$

$$\frac{\partial^2F_4}{\partial T\,\partial B_\beta} = \frac{1}{F_4}\left(\frac{\partial F_4}{\partial T}\right)\left(\frac{\partial F_4}{\partial N_\beta}\right) + F_4\left\{\left[\frac{\tau''}{\tau} - \left(\frac{\tau'}{\tau}\right)\right]^2\left(\frac{\partial x}{\partial T}\right)\left(\frac{\partial x}{\partial N_\beta}\right) + \left(\frac{\tau'}{\tau}\right)\frac{\partial^2x}{\partial T\,\partial N_\beta} - \frac{3Z_\beta^2N_e\theta'_e}{2(\sum_\alpha N_\alpha Z_\alpha^2\theta_\alpha)^2}\frac{\partial\eta}{\partial T}\right\}, \qquad \beta \neq e\,; \tag{A43}$$

$$\frac{\partial^2F_4}{\partial V\,\partial N_\beta} = \frac{1}{F_4}\left(\frac{\partial F_4}{\partial V}\right)\left(\frac{\partial F_4}{\partial N_\beta}\right) + F_4\left\{\left[\frac{\tau''}{\tau} - \left(\frac{\tau'}{\tau}\right)^2\right]\left(\frac{\partial x}{\partial V}\right)\left(\frac{\partial x}{\partial N_\beta}\right) + \left(\frac{\tau'}{\tau}\right)\frac{\partial^2x}{\partial V\,\partial N_\beta} - \frac{3Z_\beta^2N_e\theta'_e}{2(\sum_\alpha N_\alpha Z_\alpha^2\theta_\alpha)^2}\frac{\partial\eta}{\partial V}\right\}, \qquad \beta \neq e\,; \tag{A44}$$

$$\begin{aligned}\frac{\partial^2F_4}{\partial T\,\partial N_e} = \frac{1}{F_4}\left(\frac{\partial F_4}{\partial T}\right)\left(\frac{\partial F_4}{\partial N_e}\right) + F_4\Bigg\{\left[\frac{\tau''}{\tau} - \left(\frac{\tau'}{\tau}\right)^2\right]\left(\frac{\partial x}{\partial T}\right)\left(\frac{\partial x}{\partial N_e}\right) + \left(\frac{\tau'}{\tau}\right)\frac{\partial^2x}{\partial T\,\partial N_e}\\ + \frac{3}{2\sum_\alpha N_\alpha Z_\alpha^2\theta_\alpha}\left[N_e\theta''_e\frac{\partial\eta}{\partial T}\frac{\partial\eta}{\partial N_e} + \theta'_e\left(N_e\frac{\partial^2\eta}{\partial N_e\,\partial T} + \frac{\partial\eta}{\partial T}\right) - \frac{\theta_e + N_e\theta'_e(\partial\eta/\partial N_e)}{\sum_\alpha N_\alpha Z_\alpha^2\theta_\alpha}N_e\theta'_e\frac{\partial\eta}{\partial T}\right]\Bigg\}\,;\end{aligned} \tag{A45}$$

$$\begin{aligned}\frac{\partial^2 F_4}{\partial V\,\partial N_e} &= \frac{1}{F_4}\left(\frac{\partial F_4}{\partial V}\right)\left(\frac{\partial F_4}{\partial N_e}\right) + F_4\left\{\left[\frac{\tau''}{\tau} - \left(\frac{\tau'}{\tau}\right)^2\right]\left(\frac{\partial x}{\partial V}\right)\left(\frac{\partial x}{\partial N_e}\right) + \left(\frac{\tau'}{\tau}\right)\frac{\partial^2 x}{\partial V\,\partial N_e}\right. \\ &\left. + \frac{3}{2\sum_\alpha N_\alpha Z_\alpha^2 \theta_\alpha}\left[N_e \theta_e'' \frac{\partial \eta}{\partial V}\frac{\partial \eta}{\partial N_e} + \theta_e'\left(N_e \frac{\partial^2 \eta}{\partial N_e \partial V} + \frac{\partial \eta}{\partial V}\right) - \frac{\theta_e + N_e \theta_e'(\partial\eta/\partial N_e)}{\sum_\alpha N_\alpha Z_\alpha^2 \theta_\alpha} N_e \theta_e' \frac{\partial \eta}{\partial V}\right]\right\} . \end{aligned} \tag{A46}$$

Here

$$\frac{\partial x}{\partial T} = x\left\{-\frac{3}{2T} + \left[\theta - \frac{3F_{1/2}(\eta)}{2F_{3/2}(\eta)} + \frac{N_e \theta_e'}{2\sum_\alpha N_\alpha Z_\alpha^2 \theta_\alpha}\right]\frac{\partial \eta}{\partial T}\right\} ; \tag{A47}$$

$$\frac{\partial x}{\partial V} = x\left\{-\frac{1}{2V} + \left[\theta - \frac{3F_{1/2}(\eta)}{2F_{3/2}(\eta)} + \frac{N_e \theta_e'}{2\sum_\alpha N_\alpha Z_\alpha^2 \theta_\alpha}\right]\frac{\partial \eta}{\partial V}\right\} ; \tag{A48}$$

$$\begin{aligned}\frac{\partial^2 x}{\partial T^2} &= \frac{1}{x}\left(\frac{\partial x}{\partial T}\right)^2 + x\bigg[\!\!\bigg[\frac{3}{2T^2} + \left[\theta_e - \frac{3F_{1/2}(\eta)}{2F_{3/2}(\eta)} + \frac{N_e \theta_e'}{2\sum_\alpha N_\alpha Z_\alpha^2 \theta_\alpha}\right]\frac{\partial^2 \eta}{\partial T^2} \\ &+ \left\{\theta_e' - \frac{3F_{1/2}(\eta)}{2F_{3/2}(\eta)}\left[\theta_e - \frac{3F_{1/2}(\eta)}{2F_{3/2}(\eta)}\right] + \frac{N_e}{2\sum_\alpha N_\alpha Z_\alpha^2 \theta_\alpha}\left(\theta_e'' - \frac{N_e \theta_e'^2}{\sum_\alpha N_\alpha Z_\alpha^2 \theta_\alpha}\right)\right\}\left(\frac{\partial \eta}{\partial T}\right)^2\bigg]\!\!\bigg] , \end{aligned} \tag{A49}$$

$$\begin{aligned}\frac{\partial^2 x}{\partial T\,\partial V} &= \frac{1}{x}\left(\frac{\partial x}{\partial T}\right)\left(\frac{\partial x}{\partial V}\right) + x\bigg[\!\!\bigg[\left[\theta_e - \frac{3F_{1/2}(\eta)}{2F_{3/2}(\eta)} + \frac{N_e \theta_e'}{2\sum_\alpha N_\alpha Z_\alpha^2 \theta_\alpha}\right]\frac{\partial^2 \eta}{\partial T\,\partial V} \\ &+ \left\{\theta_e' - \frac{3F_{1/2}(\eta)}{2F_{3/2}(\eta)}\left[\theta_e - \frac{3F_{1/2}(\eta)}{2F_{3/2}(\eta)}\right] + \frac{N_e}{2\sum_\alpha N_\alpha Z_\alpha^2 \theta_\alpha}\left(\theta_e'' - \frac{N_e \theta_e'^2}{\sum_\alpha N_\alpha Z_\alpha^2 \theta_\alpha}\right)\right\}\left(\frac{\partial \eta}{\partial T}\right)\left(\frac{\partial \eta}{\partial V}\right)\bigg]\!\!\bigg] ; \end{aligned} \tag{A50}$$

$$\begin{aligned}\frac{\partial^2 x}{\partial V^2} &= \frac{1}{x}\left(\frac{\partial x}{\partial V}\right)^2 + x\bigg[\!\!\bigg[\frac{1}{2V^2} + \left[\theta_e - \frac{3F_{1/2}(\eta)}{2F_{3/2}(\eta)} + \frac{N_e \theta_e'}{2\sum_\alpha N_\alpha Z_\alpha^2 \theta_\alpha}\right]\frac{\partial^2 \eta}{\partial V^2} \\ &+ \left\{\theta_e' - \frac{3F_{1/2}(\eta)}{2F_{3/2}(\eta)}\left[\theta_e - \frac{3F_{1/2}(\eta)}{2F_{3/2}(\eta)}\right] + \frac{N_e}{2\sum_\alpha N_\alpha Z_\alpha^2 \theta_\alpha}\left(\theta_e'' - \frac{N_e \theta_e'^2}{\sum_\alpha N_\alpha Z_\alpha^2 \theta_\alpha}\right)\right\}\left(\frac{\partial \eta}{\partial V}\right)^2\bigg]\!\!\bigg] ; \end{aligned} \tag{A51}$$

$$\frac{\partial^2 x}{\partial T \partial N_\beta} = \frac{1}{x}\left(\frac{\partial x}{\partial T}\right)\left(\frac{\partial x}{\partial N_\beta}\right) - \frac{x Z_\beta^2 N_e \theta_e'}{2(\sum_\alpha N_\alpha Z_\alpha^2 \theta_\alpha)^2}\left(\frac{\partial \eta}{\partial T}\right) , \qquad \beta \neq e ; \tag{A52}$$

$$\frac{\partial^2 x}{\partial V \partial N_\beta} = \frac{1}{x}\left(\frac{\partial x}{\partial V}\right)\left(\frac{\partial x}{\partial N_\beta}\right) - \frac{x Z_\beta^2 N_e \theta_e'}{2(\sum_\alpha N_\alpha Z_\alpha^2 \theta_\alpha)^2}\left(\frac{\partial \eta}{\partial V}\right) , \qquad \beta \neq e ; \tag{A53}$$

$$\begin{aligned}\frac{\partial^2 x}{\partial T\,\partial N_e} &= \frac{1}{x}\left(\frac{\partial x}{\partial T}\right)\left(\frac{\partial x}{\partial N_e}\right) + x\bigg[\!\!\bigg[-\frac{3F_{1/2}(\eta)}{2F_{3/2}(\eta)}\left\{\frac{\partial^2 \eta}{\partial T\,\partial N_e} + \left[\theta_e - \frac{3F_{1/2}(\eta)}{2F_{3/2}(\eta)}\right]\left(\frac{\partial \eta}{\partial N_e}\right)\left(\frac{\partial \eta}{\partial T}\right)\right\} \\ &+ \frac{1}{2\sum_\alpha N_\alpha Z_\alpha^2 \theta_\alpha}\left[N_e \theta_e''\left(\frac{\partial \eta}{\partial T}\right)\left(\frac{\partial \eta}{\partial N_e}\right) + \theta_e'\left(\frac{\partial \eta}{\partial T} + N_e \frac{\partial^2 \eta}{\partial T\,\partial N_e}\right) - \frac{\theta_e + N_e \theta_e'(\partial\eta/\partial N_e)}{\sum_\alpha N_\alpha Z_\alpha^2 \theta_\alpha} N_e \theta_e' \frac{\partial \eta}{\partial T}\right]\bigg]\!\!\bigg] ; \end{aligned} \tag{A54}$$

and

$$\begin{aligned}\frac{\partial^2 x}{\partial V\,\partial N_e} &= \frac{1}{x}\left(\frac{\partial x}{\partial V}\right)\left(\frac{\partial x}{\partial N_e}\right) + x\bigg[\!\!\bigg[-\frac{3F_{1/2}(\eta)}{2F_{3/2}(\eta)}\left\{\frac{\partial^2 \eta}{\partial V\,\partial N_e} + \left[\theta_e - \frac{3F_{1/2}(\eta)}{2F_{3/2}(\eta)}\right]\left(\frac{\partial \eta}{\partial N_e}\right)\left(\frac{\partial \eta}{\partial V}\right)\right\} \\ &+ \frac{1}{2\sum_\alpha N_\alpha Z_\alpha^2 \theta_\alpha}\left[N_e \theta_e''\left(\frac{\partial \eta}{\partial V}\right)\left(\frac{\partial \eta}{\partial N_e}\right) + \theta_e'\left(\frac{\partial \eta}{\partial V} + N_e \frac{\partial^2 \eta}{\partial V\,\partial N_e}\right) - \frac{\theta_e + N_e \theta_e'(\partial\eta/\partial N_e)}{\sum_\alpha N_\alpha Z_\alpha^2 \theta_\alpha} N_e \theta_e' \frac{\partial \eta}{\partial V}\right]\bigg]\!\!\bigg] . \end{aligned} \tag{A55}$$

Other derivatives not defined here are given in Appendix A of Paper II.

V. FREE ENERGY OF RADIATION

$$F_R = -\tfrac{1}{3} a T^4 V ; \tag{A56}$$

$$E_R = a T^4 V ; \tag{A57}$$

$$P_R = \tfrac{1}{3} a T^4 ; \tag{A58}$$

$$\frac{\partial^2 F_R}{\partial T^2} = -4 a T^2 V ; \tag{A59}$$

$$\frac{\partial^2 F_R}{\partial T\,\partial V} = -\frac{4}{3} a T^3 ; \tag{A60}$$

$$\frac{\partial^2 F_R}{\partial V^2} \equiv 0\,; \tag{A61}$$

$$\frac{\partial^2 F_R}{\partial N_s \partial T} = \frac{\partial^2 F_R}{\partial N_s \partial V} \equiv 0\,. \tag{A62}$$

VI. FREE ENERGY OF PRESSURE IONIZATION TERM

$$\frac{\partial F'}{\partial T} = -k \sum_{\nu} N_\nu \ln \Psi_\nu\,; \tag{A63}$$

$$\frac{\partial F'}{\partial V} = -kT \sum_{\nu} N_\nu \frac{\partial \ln \Psi_\nu}{\partial V}\,; \tag{A64}$$

$$\frac{\partial^2 F'}{\partial T^2} \equiv 0\,; \tag{A65}$$

$$\frac{\partial^2 F'}{\partial T\, \partial V} = -k \sum_{\nu} N_\nu \frac{\partial \ln \Psi_\nu}{\partial V}\,; \tag{A66}$$

$$\frac{\partial^2 F'}{\partial V^2} = -kT \sum_{\nu} N_\nu \frac{\partial^2 \ln \Psi_\nu}{\partial V^2}\,; \tag{A67}$$

$$\frac{\partial^2 F'}{\partial T\, \partial N_\nu} = -k\left(\ln \Psi_\nu + \sum_{\mu} N_\mu \frac{\partial \ln \Psi_\mu}{\partial N_\nu}\right), \tag{A68}$$

and

$$\frac{\partial^2 F'}{\partial V\, \partial N_\nu} = -kT\left(\frac{\partial \ln \Psi_\nu}{\partial V} + \sum_{\mu} N_\mu \frac{\partial^2 \ln \Psi_\mu}{\partial V\, \partial N_\nu}\right), \tag{A69}$$

where

$$\frac{\partial \ln \Psi_\nu}{\partial V} = \frac{-n \ln \Psi_\nu}{V}, \tag{A70}$$

$$\frac{\partial^2 \ln \Psi_\nu}{\partial V^2} = \frac{-(n+1)}{V} \frac{\partial \ln \Psi_\nu}{\partial V}, \tag{A71}$$

and

$$\frac{\partial^2 \ln \Psi_\nu}{\partial V\, \partial N_\nu} = -\frac{n}{V} \frac{\partial \ln \Psi_\nu}{\partial N_\nu}\,. \tag{A72}$$

REFERENCES

Carlson, R. E., and Fritsch, F. N. 1985, *SIAM J. Numer. Anal.*, **22**, 386.
Cox, J. P., and Giuli, R. T. 1968, *Principles of Stellar Structure* (New York: Gordon & Breach).
Fontaine, G., Graboske, H. C., and Van Horn, H. M. 1977, *Ap. J. Suppl.*, **35**, 293.
Graboske, H. C., Harwood, D. J., and Rogers, F. J. 1969, *Phys. Rev.*, **186**, 210.
Hummer, D. G., and Mihalas, D. 1988, *Ap. J.*, **331**, 794 (Paper I).
Mihalas, D., Däppen, W., and Hummer, D. G. 1988, *Ap. J.*, **331**, 815 (Paper II).
Reichl, L. E. 1980, *A Modern Course in Statistical Physics* (London: Arnold).

W. DÄPPEN: Observatoire de Paris-Meudon, 92195 Meudon, France

D. G. HUMMER and D. MIHALAS: Joint Institute for Laboratory Astrophysics, University of Colorado, Boulder, CO 80309

B. W. MIHALAS: National Center for Supercomputing Applications, University of Illinois, 605 E. Springfield Ave., Champaign, IL 61820